SINGULARLY PERTURBED PERIODIC PARABOLIC EQUATIONS WITH ALTERNATING BOUNDARY LAYER TYPE SOLUTIONS IN SPATIALLY TWO-DIMENSIONAL DOMAINS

ADELAIDA B. VASIL'EVA* AND LEONID V. KALACHEV†

Abstract. In this article we continue the analysis of a class of singularly perturbed parabolic equations with alternating boundary layer type solutions. For such problems the degenerate (reduced) equations obtained by setting small parameter equal to zero correspond to algebraic equations that have several isolated roots. As time increases, solutions of these equations periodically go through two comparatively long lasting stages with fast transitions between these stages. During one of these stages the solution outside the boundary layer (i.e., the regular part of the asymptotic solution) is close to one of the roots of the degenerate equation. During the other stage the regular part of the asymptotic solution is close to the other root. Here we discuss some specific features of solutions' behavior for such problems in certain two-dimensional spatial domains.

Key words. singular perturbations, parabolic equations, boundary function method, two-dimensional spatial domains

AMS subject classifications. 34E10, 35B05, 35B25

1. Introduction. Singularly perturbed parabolic equations in bounded one-dimensional spatial domains (i.e., on finite segments) with alternating boundary layer type solutions were studied in a number of publications (see, e.g., Vasil'eva [2], Vasil'eva et al. [7], [6], and Vasil'eva and Kalachev [4], [5]). Here we present a number of results on qualitative asymptotic analysis of alternating boundary layer type solutions of the bistable scalar parabolic equations with periodic dependence on time variable in spatially two-dimensional domains (rings and rectangles). For the cases of ring shaped domains (similar analysis is easily extended to disk shaped domains) we show how such solutions appear under additional assumption that the non-linearity in the equation does not contain explicit dependence on spatial variables. We use computational experiments to illustrate some special features of solutions' behavior that appear in the cases where the spatial domain of interest has a shape of a rectangle. Similar to spatially one-dimensional case, for the case of two-dimensional domains the solutions of mentioned above singularly perturbed parabolic equations periodically go through two comparatively long lasting stages with fast transitions between them. During these long lasting stages the solutions outside the boundary layer are close to different roots of the nonlinear term in the equation (the term that does not contain derivatives). The main analytical techniques used in the study are (a) the *boundary function method* algorithm (see Vasil'eva et al. [3]) and (b) the *phase-plane analysis* of the trajectories (in corresponding phase planes) describing solution behavior in the boundary layers near the boundaries of spatially two-dimensional domains.

In spatially one-dimensional cases, when the right hand side of the parabolic equation does not depend explicitly on a spatial variable, the moving thresholds that represent transitions from one type of boundary layer type solution (e.g., upper solution) to another (e.g., lower solution) start symmetrically on both sides of the spatial interval (segment). This is not any more the case when we consider the same equation in spatially two-dimensional domain that has a shape of a ring. We will explain

*Department of Physics, Moscow State University, Moscow, 119899 Russia (abvas@mathabv.phys.msu.su).

†Department of Mathematical Sciences, University of Montana, Missoula, MT 59812, USA (kalachev@mso.umt.edu).

why in the case of ring shaped domains the transition will always start at the outer boundary of the ring (i.e., at the circular boundary with greater radius).

Here we do not discuss the structure of the fast moving transition layers that accompany switching between the two mentioned above longer lasting stages of the periodic solution. One may find a more detailed description of the periodic traveling waves for reaction-diffusion equations, e.g., in Alikakos et al. [1]; see also Vasil'eva et al. [7], and Vasil'eva and Kalachev [4].

The paper is organized as follows. In Section 2 we present a statement of the original problem in the ring shaped domain, briefly review previous results on constructing *alternating boundary layer type solutions* for singularly perturbed parabolic equations in one-dimensional spatial domains, analyze the original problem in the two-dimensional domain emphasizing the differences in the analysis that appear due to increase in the number of spatial dimensions. We also present some illustrative numerical computation results. In Section 3 we show numerical computation results for the problem in a rectangular domain, as well as briefly comment on the new features of solution behavior characteristic of this case. Finally, a brief conclusion is presented in Section 4.

2. Boundary layer type periodic solutions of singularly perturbed parabolic equations in a ring.

2.1. Statement of the problem in a ring shaped domain. Let us consider a radially symmetric boundary value problem for parabolic equation in a ring (here $0 < \varepsilon \ll 1$ is a small parameter):

$$\varepsilon^2(\Delta u - u_t) = \varepsilon^2 \left(\frac{\partial^2 u}{\partial r^2} + \frac{1}{r}\frac{\partial u}{\partial r} - \frac{\partial u}{\partial t} \right) = (u^2 - 1)(u - \phi(t)) = F(u,t), \tag{2.1}$$

$$r_0 < r < r_1,$$

with Dirichlet type boundary conditions and periodic conditions in t:

$$u(r_0, t, \varepsilon) = u(r_1, t, \varepsilon) = 0, \tag{2.2}$$

$$u(r, t, \varepsilon) = u(r, t + 2\pi, \varepsilon). \tag{2.3}$$

Here $-1 < \phi(t) < 1$ is a 2π-periodic function of t. Although the form of this periodic function $\phi(t)$ could be quite general, without loss of generality, and strictly for illustrative purposes, a particular choice of $\phi(t)$ for quantitative and computational examples will be made later.

2.2. Review of the results for spatially one-dimensional case. To better understand what happens in the case of problem (2.1) – (2.3), first, we review the results related to a similar problem for parabolic equation in a spatially one-dimensional domain (e.g., we consider a segment $[0, 1]$) with Dirichlet type boundary conditions and periodic conditions in t (see Vasil'eva and Kalachev [4]):

$$\varepsilon^2(u_{xx} - u_t) = (u^2 - 1)(u - \phi(t)) = F(u,t), \quad 0 < x < 1, \tag{2.4}$$

$$u(0, t, \varepsilon) = u(1, t, \varepsilon) = 0, \tag{2.5}$$

$$u(x,t,\varepsilon) = u(x,t+2\pi,\varepsilon). \tag{2.6}$$

Comparing (2.1) – (2.3) with (2.4) – (2.6) we see that both problems turn out to be essentially one-dimensional, but in (2.1) instead of differential operator u_{xx} we have operator $u_{rr} + u_r/r$.

It follows from Vasil'eva and Kalachev [4] that for certain values from range of $\phi(t)$ the problem (2.4) – (2.6) may have one of the two boundary layer type solutions with the following asymptotic representations (see Figure 1):

$$u^+ = 1 + \Pi^+(\xi_0,t) + R^+(\xi_1,t) + O(\varepsilon) = \tilde{u}^+ + O(\varepsilon), \tag{2.7}$$

$$u^- = -1 + \Pi^-(\xi_0,t) + R^-(\xi_1,t) + O(\varepsilon) = \tilde{u}^- + O(\varepsilon). \tag{2.8}$$

Here $\xi_0 = x/\varepsilon$, $\xi_1 = (x-1)/\varepsilon$ are the, so-called, stretched variables; Π^+, R^+ and Π^-, R^- are the, so-called, *boundary functions* that introduce corrections to the leading order *regular* terms of the asymptotic approximation $\bar{u}_1 = 1$ and $\bar{u}_3 = -1$ (two of the three solutions of the degenerate equation $(\bar{u}^2 - 1)(\bar{u} - \phi(t)) = 0$ that is obtained from (2.4) when ε is set to zero; one more solution is $\bar{u}_2 = \phi(t)$), so that the main terms of the asymptotic formulas (2.7) and (2.8), respectively, could satisfy the imposed boundary conditions in the leading order approximation. We call u^+ the *upper* boundary layer type solution, and call u^- the *lower* boundary layer type solution. We use tilde ($\tilde{}$) in (2.7), (2.8) and below to distinguish between $u^\pm$ and their leading order approximations $\tilde{u}^\pm$.

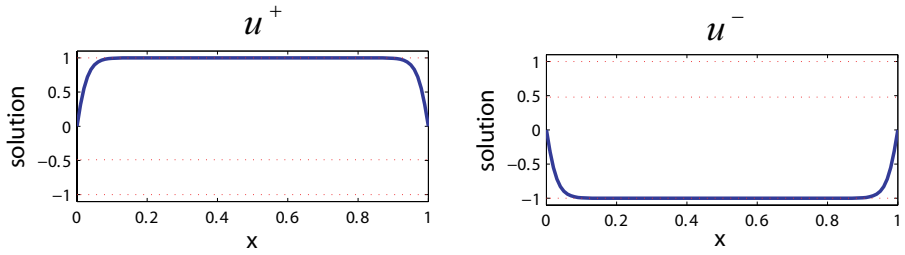

(a) (b)

Figure 1. (a) Upper solution phase. (b) Lower solution phase.

In the vicinity of $x = 0$ the upper solution of (2.4) – (2.6) is approximately described by the following equation (here t enters as a parameter):

$$\frac{d^2\tilde{u}^+}{d\xi_0^2} = F(\tilde{u}^+,t),$$
$$\tilde{u}^+(0,t) = 0, \quad \tilde{u}^+(\infty,t) = 1, \quad \tilde{u}^+(\xi_0,t+2\pi) = \tilde{u}^+(\xi_0,t). \tag{2.9}$$

The same solution in the vicinity of $x = 1$ is approximately described as follows:

$$\frac{d^2\tilde{u}^+}{d\xi_1^2} = F(\tilde{u}^+,t),$$
$$\tilde{u}^+(0,t) = 0, \quad \tilde{u}^+(-\infty,t) = 1, \quad \tilde{u}^+(\xi_1,t+2\pi) = \tilde{u}^+(\xi_1,t). \tag{2.10}$$

The boundary layer functions Π^+ and R^+ are related to the leading order approximations of the upper solution defined by (2.9) and (2.10) via the expressions:

$$\begin{aligned} &\text{near} \quad x=0, \quad \tilde{u}^+(\xi_0,t,\varepsilon)=1+\Pi^+(\xi_0,t),\\ &\text{near} \quad x=1, \quad \tilde{u}^+(\xi_1,t,\varepsilon)=1+R^+(\xi_1,t). \end{aligned} \tag{2.11}$$

For approximations of $\tilde{u}^-$ near the boundaries $x=0$, $x=1$ we can write equations similar to (2.9), (2.10), as well as functional relations similar to (2.11). In what follows, we will also use the name *boundary layer function* for approximations (2.11) of the upper function u^+ near $x=0$ and $x=1$, and for similar approximations of the lower function u^- near $x=0$ and $x=1$. These "new" boundary layer functions differ from the originally defined boundary layer functions $\Pi^\pm$, $R^\pm$ by additive constants.

Let us consider a particular choice of $\phi(t)=0.8\sin(t)$. Assume that the upper solution u^+ (see Figure 1(a)) is observed at a certain instant of time $t=t_0$. To study corresponding boundary layers, let us introduce a phase plane $(\tilde{u}^+,\tilde{z}^+)$ for equation (2.9), $d^2\tilde{u}^+/d\xi_0^2=F(\tilde{u}^+,t)$.

The first integral of this equation has the form:

$$\frac{(\tilde{z}^+)^2}{2}=\int_1^{\tilde{u}^+}(s^2-1)(s-\phi(t))ds, \tag{2.12}$$

where $\tilde{z}^+=d\tilde{u}^+/d\xi_0$. From (2.12), we obtain:

$$\frac{(\tilde{z}^+)^2}{2}=(\tilde{u}^+-1)^2\cdot\left[\frac{1}{4}(\tilde{u}^++1)-\frac{\phi(t)}{3}(\tilde{u}^++2)\right]. \tag{2.13}$$

Expressions (2.12), (2.13) are needed to study $\tilde{u}^+$ (approximation to u^+). To analyze $\tilde{u}^-$ (approximation to u^-), in (2.12) we must take the low limit of integration equal to -1 (instead of 1), and re-write this equation in terms of $\tilde{z}^-$ and $\tilde{u}^-$ instead of $\tilde{z}^+$ and $\tilde{u}^+$.

Depending on the value of t, the phase trajectory of (2.9) describing the behavior of the upper solution near the left boundary (in the left boundary layer) on $(\tilde{u}^+,\tilde{z}^+)$-phase plane may have different forms (see Figure 2).

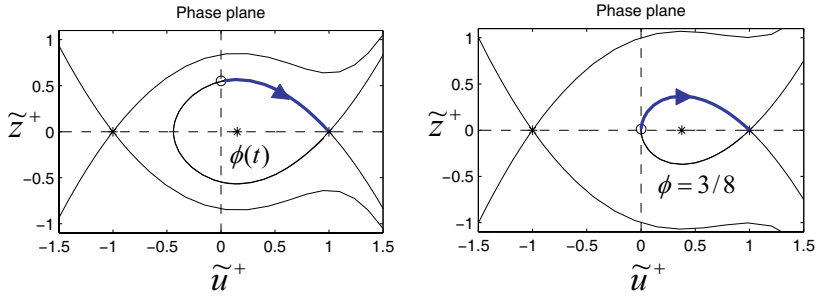

(a) (b)

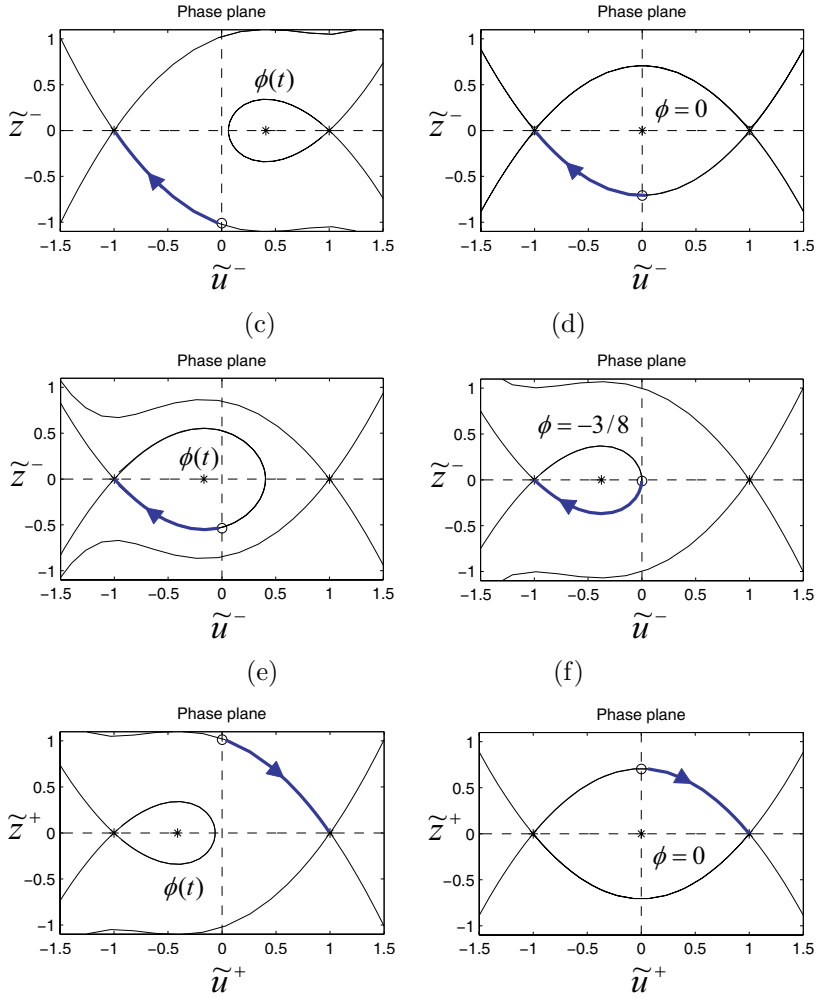

Figure 2. Bold curve on the phase plane indicates the trajectory corresponding to the left boundary layer function; arrow shows the change along the trajectory that corresponds to increasing $\xi_0 > 0$. The following cases are illustrated: (a) $\phi(t) > 0$ for some $t < t^*$; (b) $\phi(t) = 3/8$ at $t = t^*$; (c) $\phi(t) > 0$ for some $t^* < t < t^{**}$; (d) $\phi(t) = 0$ for some $t^* < t < t^{**}$; (e) $\phi(t) < 0$ for some $t < t^{**}$; (f) $\phi(t) = -3/8$ at $t = t^{**}$; (g) $\phi(t) < 0$ for some $t > t^{**}$; (h) $\phi(t) = 0$ for some $t > t^{**}$.

For the solution of problem (2.9) to exist, the straight line $\tilde{u}^+ = 0$, corresponding to the boundary condition value $\tilde{u}^+(0,t) = 0$, must intersect in the phase plane the separatrix entering saddle equilibrium (1,0) at some point $(0, \tilde{z}^+(0,t))$. One such case is shown in Figure 2(a), but this situation is not observed, e.g., in Figure 2(c). For our choice of $\phi(t) = 0.8\sin(t)$, consider the behavior of solution when $t > t_0 > 0$ increases (here t_0 is an arbitrarily chosen initial time point).

Assume that at $t = t_0 > 0$ the *upper* solution shown in Figure 1(a) is observed, and $\phi(t)$ is increasing at $t = t_0$. The phase trajectory (for the chosen initial instant of time) corresponding to the left upper boundary layer function is shown in Figure 2(a) as a bold solid line; arrow shows the direction corresponding to increasing values

of ξ_0. As t increases, it reaches some value $t = t^*$ for which the homoclinic loop trajectory that emerges from and eventually enters the same saddle equilibrium $(1, 0)$ has exactly one point of intersection with the vertical line $\tilde{u}^+ = 0$. This situation is depicted in Figure 2(b). We note that for $t = t^* + \Delta$, where Δ any small positive number, there will be no intersection between the homoclinic loop and the vertical line corresponding to boundary condition $\tilde{u}^+(0, t) = 0$. Thus, the corresponding boundary layer function, and consequently, the *upper* boundary layer type solution will cease to exist. However, the *lower* boundary layer type solution will exist for such value of t since the separatrix that enters the saddle point $(-1, 0)$ (and that describes the left boundary layer function for the *lower* solution) does intersect the vertical line $\tilde{u}^- = 0$ for some time interval with $t > t^*$. The illustration of this fact is shown in Figure 2(c). The trajectory corresponding to the left lower boundary layer function, which is a solution of equation analogous to (2.10), is depicted as a bold solid line; arrow shows the direction corresponding to increasing values of ξ_0. At $t = t^*$ the transition from *upper* to *lower* solution via moving thresholds begins simultaneously at the left and the right boundaries of the segment $[0, 1]$ (due to the fact that the problems for the left and the right upper boundary functions are similar, the conditions for their existence are violated at the same $t = t^*$). The value of t^* can be easily found from (2.13) by setting $\tilde{u}^+ = 0$, $\tilde{z}^+ = 0$, and arriving at the equation for t^*: $\phi(t^*) = 3/8$.

As t continues to increase beyond t^*, periodic function $\phi(t)$ reaches its maximum, and then starts to decrease. In Figure 2(d) we show the case where $\phi(t) = 0$, and the, so-called, cell is formed (two heteroclinic orbits connecting saddle points $(1, 0)$ and $(-1, 0)$ are observed). In Figures 2(e), 2(f) we show the cases where $\phi(t) < 0$; the situation in Figure 2(f) corresponds to the instant of time $t = t^{**}$, for which the homoclinic loop trajectory entering the saddle point $(-1, 0)$ as $\xi_0 \to \infty$ has only one point of intersection with the vertical line $\tilde{u}^- = 0$ that represents the boundary condition at $x = 0$. For $t = t^{**} + \Delta$, where Δ any small positive number, there will be no intersection between this homoclinic loop and the mentioned above vertical line. Corresponding boundary layer function, and thus, the *lower* boundary layer type solution, will not exist any more. At $t = t^{**}$ the transition from the *lower* to the *upper* solution via moving threshold begins simultaneously at the left and the right boundaries of the segment $[0, 1]$. The value of t^{**} is found from equation similar to that for t^*: it is the first solution of $\phi(t^{**}) = 3/8$ satisfying $t^{**} > t^*$.

In Figure 2(g) we show the phase trajectory (for some instant of time $t > t^{**}$) corresponding to left upper boundary layer function that connects the point representing the boundary condition (at this point $\tilde{u}^+(0, t) = 0$) with the saddle point $(1, 0)$, which corresponds to the leading order regular part of the asymptotics corresponding to *upper* solution case. As t continues to increase beyond t^{**}, periodic function $\phi(t)$ reaches its minimum, and then starts to increase. In Figure 2(h) we show the case where $\phi(t) = 0$, and once again the, so-called, cell is formed. As t continues to increase, the solution periodically repeats itself going consecutively through phases shown in Figures 2(a), 2(b), 2(c), etc.

The period of the solution, 2π, is the same as the period of $\phi(t)$. In Figure 3 we present solution surface $u(x, t)$ for which asymptotic representations over two distinct time intervals within solution period corresponding to upper and lower solution phases are given by (2.7), (2.8).

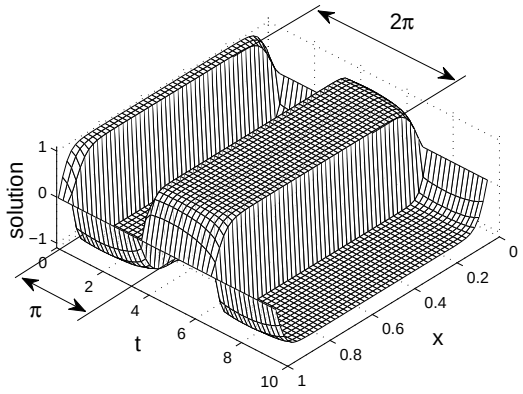

Figure 3. The surface $u = u(x,t)$ constructed numerically for some fixed small value of ε illustrates periodic switching of the solution to (2.4) – (2.6) between upper and lower solution phases.

2.3. Analysis of the original problem in a ring. Now we return to our original problem (2.1) – (2.3). Solution of this problem for certain values of $\phi(t)$ may also be either in the *upper* or in the *lower* phase. Let us introduce stretched variables $\xi_0 = (r - r_0)/\varepsilon$ and $\xi_1 = (r - r_1)/\varepsilon$. The *upper* and the *lower* boundary layer type solutions of (2.1) – (2.3) have asymptotic representations similar to (2.7) and (2.8), respectively. In the vicinity of the boundary $r = r_0$, from (2.1), we obtain:

$$\frac{\partial^2 u}{\partial \xi_0^2} + \frac{\varepsilon}{r_0 + \xi_0 \cdot \varepsilon} \cdot \frac{\partial u}{\partial \xi_0} - \varepsilon^2 \frac{\partial u}{\partial t} = (u^2 - 1)(u - \phi(t)), \quad 0 < \xi_0 < \frac{r_1 - r_0}{\varepsilon}, \tag{2.14}$$

and in the vicinity of the boundary $r = r_1$, we get:

$$\frac{\partial^2 u}{\partial \xi_1^2} + \frac{\varepsilon}{r_1 + \xi_1 \cdot \varepsilon} \cdot \frac{\partial u}{\partial \xi_1} - \varepsilon^2 \frac{\partial u}{\partial t} = (u^2 - 1)(u - \phi(t)), \quad \frac{r_0 - r_1}{\varepsilon} < \xi_1 < 0. \tag{2.15}$$

We note that the following expansions hold:

$$\frac{\varepsilon}{r_0 + \xi_0 \cdot \varepsilon} \approx \frac{\varepsilon}{r_0}\left(1 - \varepsilon\frac{\xi_0}{r_0} + \dots\right), \quad \frac{\varepsilon}{r_1 + \xi_1 \cdot \varepsilon} \approx \frac{\varepsilon}{r_1}\left(1 - \varepsilon\frac{\xi_1}{r_1} + \dots\right). \tag{2.16}$$

By virtue of (2.14) and (2.16), in the vicinity of $r = r_0$ the *upper* solution of (2.1) – (2.3) is approximately described by the following equation and conditions (here t enters as a parameter, and F is the same as in (2.9), (2.10)):

$$\begin{gathered} \frac{d^2\tilde{u}^+}{d\xi_0^2} + \frac{\varepsilon}{r_0} \cdot \frac{d\tilde{u}^+}{d\xi_0} = F(\tilde{u}^+, t), \\ \tilde{u}^+(0,t) = 0, \quad \tilde{u}^+(\infty,t) = 1, \quad \tilde{u}^+(\xi_0, t + 2\pi) = \tilde{u}^+(\xi_0, t). \end{gathered} \tag{2.17}$$

The same solution in the vicinity of $r = r_1$ is approximately described by the following problem:

$$\frac{d^2\tilde{u}^+}{d\xi_1^2} + \frac{\varepsilon}{r_1}\cdot\frac{d\tilde{u}^+}{d\xi_1} = F(\tilde{u}^+, t), \tag{2.18}$$

$$\tilde{u}^+(0,t) = 0, \quad \tilde{u}^+(-\infty,t) = 1, \quad \tilde{u}^+(\xi_1, t+2\pi) = \tilde{u}^+(\xi_1, t).$$

Similar equations and conditions may be written out for respective approximations of the *lower* solution $\tilde{u}^-$ of (2.1) – (2.3) near $r = r_0$ and $r = r_1$.

If we set $\varepsilon = 0$ in (2.17), (2.18), these equations will become (2.9), (2.10), respectively. In addition to leading order terms in (2.17), (2.18), we have to keep the terms of order $O(\varepsilon)$ since otherwise these equations cannot explain the asymmetry in the initiation of transition between the *upper* and *lower* boundary layer type solutions observed in the case of problem (2.1) – (2.3): in the case of a ring shaped domain the moving threshold that accompanies the transition always stars at the outer boundary $r = r_1 > r_0$. In the case of problem (2.4) – (2.6) due to the symmetry of equations (2.9), (2.10) (i.e., these equations do not change if we change the sign of independent variables ξ_0 and ξ_1) moving thresholds corresponding to the transitions between the *upper* and the *lower* solution phases start simultaneously (and symmetrically) at both boundaries, $x = 0$ and $x = 1$. Let us use (2.17), (2.18) to explain why the asymmetry in the initiation of transitions is observed for solutions of (2.1) – (2.3). Our approach is based on Vasil'eva and Kalachev [4], where a more detailed phase-plane analysis is presented. In what follows we use notation: $a_0 = \varepsilon/r_0 > 0$ and $a_1 = \varepsilon/r_1 > 0$. We also note that $a_0 > a_1$ since $r_0 < r_1$.

Let us start with equation from (2.18) that we re-write as follows:

$$\frac{d^2\tilde{u}^+}{d\xi_1^2} = -a_1\cdot\frac{d\tilde{u}^+}{d\xi_1} + ((\tilde{u}^+)^2 - 1)(\tilde{u}^+ - \phi(t)). \tag{2.19}$$

After computing the eigenvalues of the Jacobian matrix of the linearized version of (2.19) at the saddle point $(1, 0)$, we can find out how the directions at which separatrices emerge from or enter this saddle point change with the appearance of $a_1 > 0$ in (2.19) (compared to (2.10)). From corresponding characteristic equation obtained for (2.19) linearized near $(1, 0)$, we get (here we recall that $-1 < \phi < 1$):

$$\lambda_1 = -\frac{a_1}{2} + \sqrt{\frac{a_1^2}{4} + 2(1-\phi)} > 0, \quad \lambda_2 = -\frac{a_1}{2} - \sqrt{\frac{a_1^2}{4} + 2(1-\phi)} < 0. \tag{2.20}$$

The eigenvalues for $a_1 = 0$ are

$$\tilde{\lambda}_1 = +\sqrt{2(1-\phi)} > 0, \quad \tilde{\lambda}_2 = -\sqrt{2(1-\phi)} < 0. \tag{2.21}$$

Evidently, $0 < \lambda_1 < \tilde{\lambda}_1$ and $\lambda_2 < \tilde{\lambda}_2 < 0$. Since we consider approximation to the upper solution near $r = r_1$, in the vicinity of the saddle point $(1, 0)$ we must have

$$(\tilde{u}^+ - 1) = C\cdot\exp(\lambda_1\xi_1) \quad \text{as} \quad \xi_1 \to -\infty, \tag{2.22}$$

where $C < 0$ is some constant. Thus, corresponding

$$\tilde{z}^+ = \frac{d\tilde{u}^+}{d\xi_1} = \lambda_1\cdot C\cdot\exp(\lambda_1\xi_1) \quad \text{as} \quad \xi_1 \to -\infty, \tag{2.23}$$

and the positive slope of a tangent line to the trajectory (in the $(\tilde{u}^+, \tilde{z}^+)$-phase plane) corresponding to the boundary function near $r = r_1$ is defined as

$$\frac{d\tilde{z}^+}{d\tilde{u}^+} = \lambda_1 > 0 \quad \text{as} \quad \xi_1 \to -\infty, \tag{2.24}$$

Since $0 < \lambda_1 < \tilde{\lambda}_1$, for the ring domain the separatrix entering the saddle $(1, 0)$ and describing the boundary layer function near $r = r_1$ lies in the phase plane above corresponding separatrix describing the function in the boundary layer near $x = 1$ (for the case of one-dimensional segment $[0, 1]$). In Figure 4(a) we show the trajectories corresponding to the boundary functions near the boundary $r = r_1$ for the ring (solid line) and near the boundary $x = 1$ for the segment (dashed line).

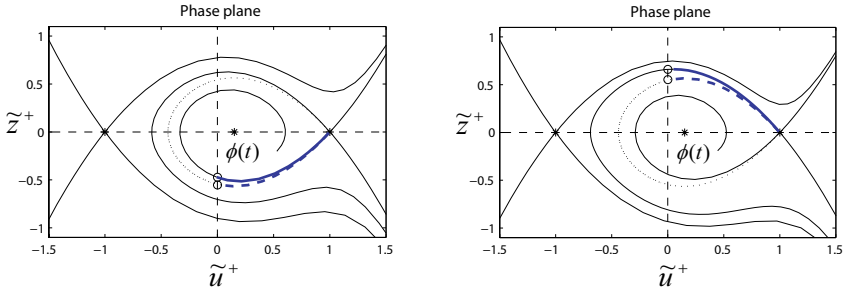

(a) (b)

Figure 4. Trajectories corresponding to the boundary functions (for the same value of $\phi(t)$) (a) near the boundary $r = r_1$ for the ring (solid line) and near the boundary $x = 1$ for the segment (dashed line); (b) near the boundary $r = r_0$ for the ring (solid line) and near the boundary $x = 0$ for the segment (dashed line).

Repeating similar analysis for equation (2.17) re-written in the form

$$\frac{d^2\tilde{u}^+}{d\xi_0^2} = -a_0 \cdot \frac{d\tilde{u}^+}{d\xi_0} + ((\tilde{u}^+)^2 - 1)(\tilde{u}^+ - \phi(t)), \tag{2.25}$$

we can derive the following relations for eigenvalues

$$\hat{\lambda}_1 = -\frac{a_0}{2} + \sqrt{\frac{a_0^2}{4} + 2(1-\phi)} > 0, \quad \hat{\lambda}_2 = -\frac{a_0}{2} - \sqrt{\frac{a_0^2}{4} + 2(1-\phi)} < 0. \tag{2.26}$$

Comparing them with the eigenvalues (2.21) computed for the case where $a_0 = 0$, we arrive at the relations: $0 < \hat{\lambda}_1 < \tilde{\lambda}_1$ and $\hat{\lambda}_2 < \tilde{\lambda}_2 < 0$. Since we now consider approximation to upper solution near $r = r_0$, in the vicinity of the saddle point $(1, 0)$ we must have

$$(\tilde{u}^+ - 1) = C \cdot \exp(\hat{\lambda}_2 \xi_0) \quad \text{as} \quad \xi_0 \to +\infty, \tag{2.27}$$

where $C < 0$ is some constant. Same as before, corresponding

$$\tilde{z}^+ = \frac{d\tilde{u}^+}{d\xi_0} = \hat{\lambda}_2 \cdot C \cdot \exp(\hat{\lambda}_2 \xi_1) \quad \text{as} \quad \xi_0 \to +\infty, \tag{2.28}$$

and the negative slope of a tangent line to the trajectory corresponding to the boundary function near $r = r_0$ is defined as

$$\frac{d\tilde{z}^+}{d\tilde{u}^+} = \hat{\lambda}_2 < 0 \quad \text{as} \quad \xi_0 \to +\infty, \tag{2.29}$$

Since $\hat{\lambda}_2 < \tilde{\lambda}_2 < 0$, for the ring shaped domain we once again have that the separatrix entering the saddle $(1, 0)$ and describing the boundary layer function near $r = r_0$ lies in the phase plane above corresponding separatrix describing the function in the boundary layer near $x = 0$ (for the case of one-dimensional segment $[0, 1]$). In Figure 4(b) we show the trajectories corresponding to the boundary functions near the boundary $r = r_0$ for the ring (solid line) and near the boundary $x = 0$ for the segment (dashed line).

As long as $0 < a_1 < a_0$, for the case of upper solution we will always have that the trajectory corresponding to boundary function defined near $r = r_0$ lies in the phase plane outside the homoclinic loop (that appears if we set $a_0 = a_1 = 0$), and that the trajectory corresponding to boundary function defined near $r = r_1$ lies inside this homoclinic loop; see Figures 4(a) and 4(b), where the mentioned above homoclinic loop is shown as a dotted curve. Thus, as t increases, at some value of $t = t^* < 3/8$ we will arrive at the situation shown in Figures 5(a) and 5(b). In Figure 5(a) the bold solid line represents the trajectory corresponding to the boundary function defined near $r = r_1$; arrow indicates the direction corresponding to decrease in ξ_1. At this instant of time $t = t^*$ the separatrix to which this trajectory belongs has just one point of intersection with the vertical line $\tilde{u}^+ = 0$ (corresponding to the boundary condition at $r = r_1$). At an instant of time $t = t^* + \Delta$, where Δ is any small positive number, there will be no more points of intersection of this separatrix with line $\tilde{u}^+ = 0$. Thus, the upper solution will cease to exist, and the transition from upper to lower solution phase via moving threshold will be initiated at the boundary $r = r_1$. However, as we can see in Figure 5(b), the trajectory describing the boundary function defined near $r = r_0$ that exists at $t = t^*$ (solid line; arrow indicates the direction corresponding to increase in ξ_0) will still exist for $t = t^* + \Delta$ for some positive Δ: the point of intersection of the separatrix entering the saddle $(1, 0)$ identified by a small circle in Figure 5(b) will not disappear for small increase in $\phi(t)$. Thus, at $t = t^*$ the transition threshold will not start at the boundary $r = r_0$.

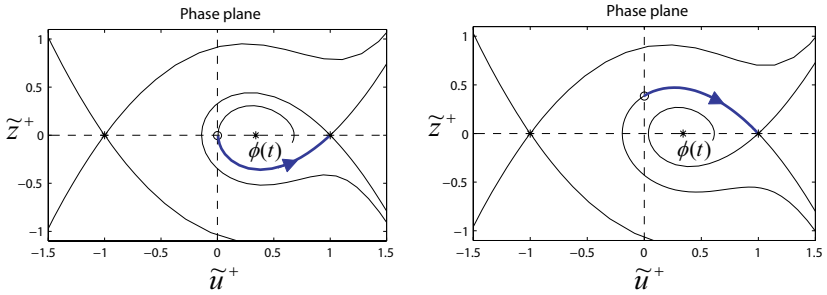

(a) (b)

Figure 5. Phase trajectories (at an instant of time $t = t^* < 3/8$) corresponding to boundary layer functions defined (a) near $r = r_1$ (arrow shows the direction of decrease in ξ_1); (b) near $r = r_0$ (arrow shows the direction of increase in ξ_0).

Here we omit the details of analysis related to initiation of transition back from *lower* to *upper* solution phase. Using the argument similar to that presented above, it can be shown that, once again, the transition via moving threshold always starts at the outer boundary $r = r_1$ of the ring shaped domain.

2.4. Results of numerical computations for the problem in a ring shaped domain. Let us illustrate the discussion presented above using the results of numerical computations performed for the original problem (2.1) – (2.3) for a particular choice of parameter values: $r_0 = 1$, $r_1 = 2$, $\varepsilon = \sqrt{0.001}$. We also use $\phi(t) = -0.7\sin(2t + \delta)$, where δ is an appropriately chosen phase shift. In Figure 6(a) we show the snapshot of the solution of the original problem in its *upper* solution phase at a certain instant of time $t > 0$. As t increases, it reaches the value $t = t^*$ (mentioned previously in the text) at which the transition from the *upper* to the *lower* phase of the solution via moving threshold starts at the outer ring boundary $r = r_1$. In Figure 6(b) we show the solution at an instant of time $t_1 > t^*$, when the moving threshold has already formed at the boundary $r = r_1$. It moves toward the inner boundary $r = r_0$. We note that for the instant of time shown in Figure 6(b) no threshold moving from $r = r_0$ toward $r = r_1$ exists. In Figure 6(c) we present the situation observed at an instant of time $t_2 > t_1$ for which, in addition to the first moving threshold, the second moving threshold (formed at the boundary $r = r_0$) is also observed. The two thresholds are moving toward each other. The transition from the *upper* to the *lower* solution phase is completed when the two thresholds meet each other at some instant of time $t_3 > t_2$. Finally, in Figure 6(d) we show the solution of the original problem in its *lower* phase that is observed for some $t > t_3$.

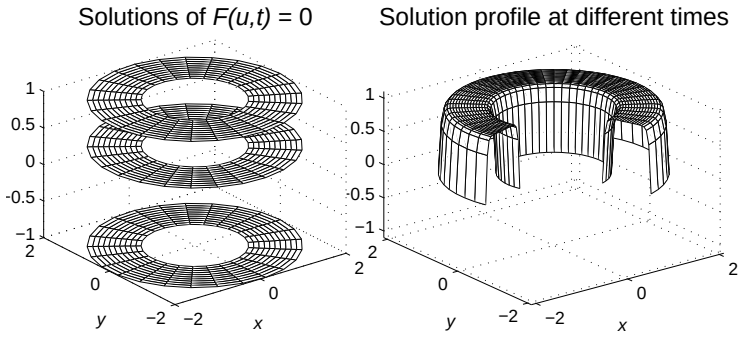

(a)

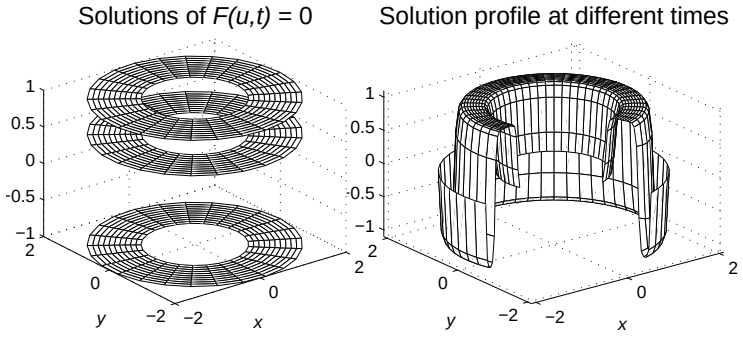

(b)

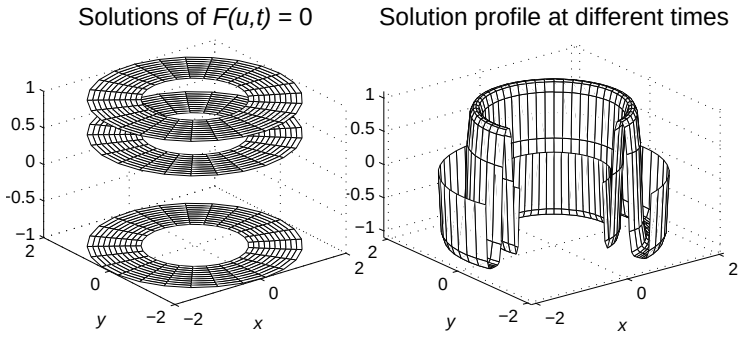

(c)

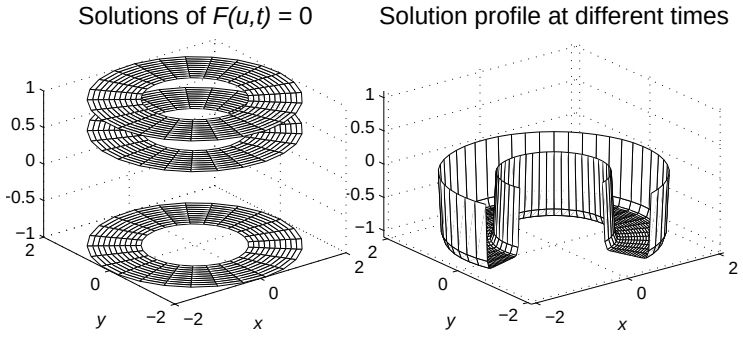

(d)

Figure 6. (a) Solution of the original problem in its *upper* phase. (b) The first moving threshold has been formed at the boundary $r = r_1$. (c) The second threshold has been formed at the boundary $r = r_0$; the thresholds move toward each other. (d) Solution of the original problem in its *lower* phase.

3. Results of numerical computations for the problem in a rectangular domain. Let us consider a particular boundary value problem for parabolic equation similar to (2.1) – (2.3) but now defined in a rectangular domain:

$$\varepsilon^2(\Delta u - u_t) = \varepsilon^2\left(\frac{\partial^2 u}{\partial x^2} + \frac{\partial^2 u}{\partial y^2} - \frac{\partial u}{\partial t}\right) = (u^2-1)(u-\phi(t)) = F(u,t), \tag{3.1}$$

$$0 < x < a, \quad 0 < y < b.$$

The Dirichlet type boundary conditions are

$$u(0,y,t,\varepsilon) = u(a,y,t,\varepsilon) = u(x,0,t,\varepsilon) = u(x,b,t,\varepsilon) = 0. \tag{3.2}$$

Periodic conditions in t are the same as before:

$$u(x,y,t,\varepsilon) = u(x,y,t+2\pi,\varepsilon). \tag{3.3}$$

Here $-1 < \phi(t) < 1$ is a 2π-periodic function of t, and $0 < \varepsilon \ll 1$ is a small parameter.

While in this paper we do not present analytical study of (3.1) – (3.3), it is instructive to discuss the features of the numerical solution of this problem obtained for the same parameter values and for the same $\phi(t)$ as those used in previous example

(for which the snapshots of the solution at various instants of time are shown in Figures 6(a)–(d)). Also we choose $a = b = 1$, i.e., the rectangular domain in this example is actually a square.

In Figure 7(a) we present the solution of the problem (3.1) – (3.3) in its *upper* phase at an instant of time $t_1 > 0$. As t increases, it eventually reaches certain value $t = \tilde{t}^*$ at which the transition from the *upper* to the *lower* phase of the solution stars. However, unlike the previous example, where the moving transition threshold started simultaneously at all the points of the ring shaped domain's outer boundary, here the transition "waves" first start at the four corners of the square shaped spatial domain; see Figure 7(b) where the solution profile is shown for an instant of time $t_2 > \tilde{t}^*$. It also follows from the numerical computation that the transition start time for the square shaped domain is smaller compared to that for the ring domain: $\tilde{t}^* < t^*$. In Figure 7(c) we show the solution at an instant of time $t_3 > t_2$ when the moving threshold is located entirely within the square domain. Finally, in Figure 7(d) we present the solution of the problem (3.1) – (3.3) in its *lower* phase that is observed for some $t > t_3$.

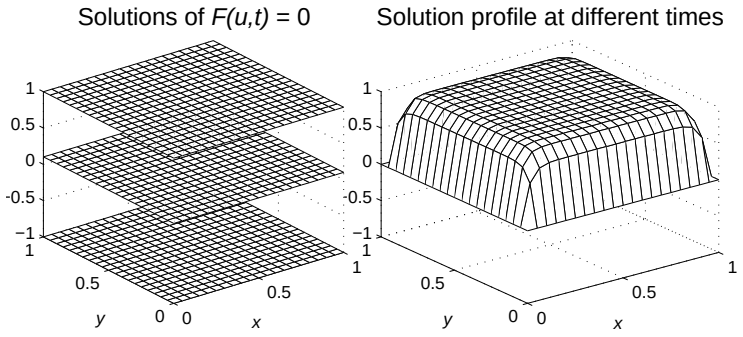

(a)

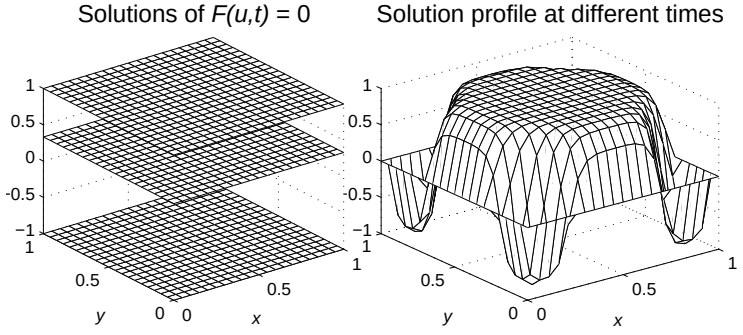

(b)

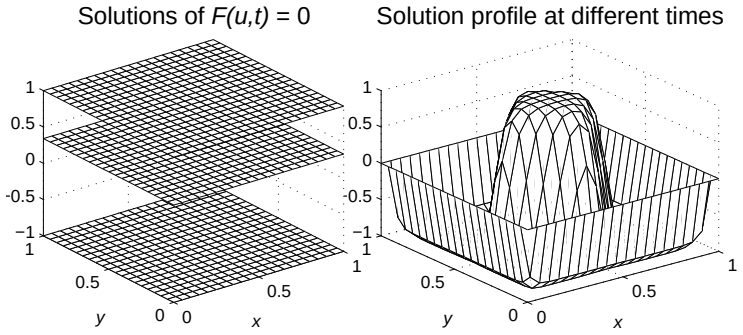

(c)

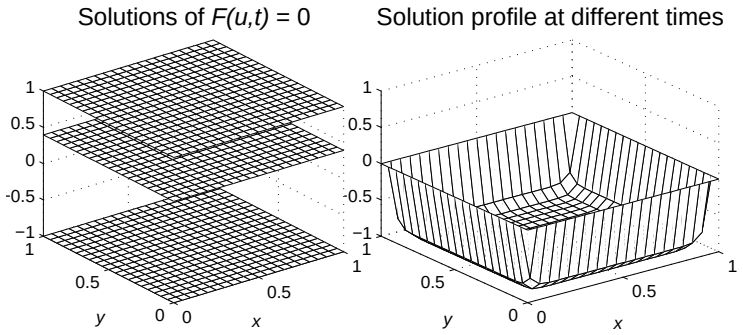

(d)

Figure 7. (a) Solution of the problem (3.1) – (3.3) in its *upper* phase. (b) The moving thresholds have been formed at the corners of the square domain. (c) Solution profile at an instant of time when the moving threshold is located entirely within the square domain. (d) Solution of the problem (3.1) – (3.3) in its *lower* phase.

The heuristic explanation of symmetry breaking in the moving threshold formation observed for the domain with corners (square) compared to the case of the domain without corners (ring) when the function in the right hand side of the equation does not depend explicitly on spatial variables and when the boundary conditions are homogeneous can be given as follows. For small enough ε in the vicinity of the sides of the square spatial domain, and away from the corners, the problem may be approximately treated (locally) as one dimensional: the conditions for existence of boundary layer functions there are similar to those that must hold for the end points of one-dimensional linear segment (see Subsection 2.2). On the other hand, in the vicinity of the corners the problem must be approximately treated as two dimensional: the corners may be considered as the limits of smooth boundaries (quarters or a circle) when their radius tends to zero (and thus, the curvature tends to infinity). The conditions for existence of the boundary functions near the corners are, thus, violated for smaller values of $\phi(t)$ compared to corresponding conditions for boundary functions near the sides of the rectangle. As a result, the moving thresholds are initiated at the corners earlier compared to those initiated at the sides.

If the right hand side of the equation or the boundary conditions depend explicitly on spatial variables, the formation and dynamics of the moving thresholds accompanying the transitions between the lower and the upper stages of the periodic solution

become much more complex. No analytical description of such transitions is currently available in the literature.

4. Conclusion. In this paper we addressed some problems for a class of periodic singularly perturbed parabolic differential equations formulated in spatially two-dimensional domains. We used perturbation approach to explain why in a ring shaped domain the transitions between the lower and the upper phases of the periodic solution always start at the outer boundary of the ring. We illustrated our findings using numerical solutions of the original problem obtained for certain particular choice of parameter values. We also provided results of computational experiments for the case of a domain that has a shape of a rectangle.

Acknowledgements. This work was supported in part by the faculty exchange grant from The University of Montana awarded to Leonid Kalachev.

REFERENCES

[1] N.D. Alikakos, P.W. Bates, and X. Chen, Periodic traveling waves and locating oscillating patterns in multidimensional domains, *Trans. AMS* 351(1999), pp. 2777 – 2805.

[2] A.B. Vasil'eva, Periodic solutions to a parabolic problem with a small parameter multiplying the derivatives, *Comput. Math. Math. Phys.* 43(2003), pp. 932 – 943.

[3] A.B. Vasil'eva, V.F. Butuzov, and L.V. Kalachev, *The Boundary Function Method for Singular Perturbation Problems*, SIAM Studies in Appl. Math., SIAM, Philadelphia,1995.

[4] A.B. Vasil'eva and L.V. Kalachev, Singularly perturbed periodic parabolic equations with alternating boundary layer type solutions, *Abstract and Applied Analysis*, Vol. 2006 (2006), Article ID 52856, 21 pages.

[5] A.B. Vasil'eva and L.V. Kalachev, Alternating boundary layer type solutions of some singularly perturbed periodic parabolic equations with Dirichlet and Robin boundary conditions, *Comput. Math. and Math. Physics.*, Vol. 47 (2) (2007), pp. 222 – 233.

[6] A.B.Vasil'eva, L.V.Kalachev, and A.A.Plotnikov, On certain control problems for a class of singularly perturbed parabolic equations, *Intl. J. Modern Math.* 2(2) (2007), pp. 177 – 190.

[7] A.B. Vasil'eva, A.P. Petrov, and A.A. Plotnikov, On the theory of alternating contrast structures, *Comput. Math. Math. Phys.* 38(1998), pp. 1471 – 1480.